Gas flow driven by thermal creep in dusty plasma

T. M. Flanagan and J. Goree
Department of Physics and Astronomy, The University of Iowa, Iowa City, Iowa 52242, USA
(Received 9 June 2009; published 13 October 2009)

Thermal creep flow (TCF) is a flow of gas driven by a temperature gradient along a solid boundary. Here, TCF is demonstrated experimentally in a dusty plasma. Stripes on a glass box are heated by laser beam absorption, leading to both TCF and a thermophoretic force. The design of the experiment allows isolating the effect of TCF. A stirring motion of the dust particle suspension is observed. By eliminating all other explanations for this motion, we conclude that TCF at the boundary couples by drag to the bulk gas, causing the bulk gas to flow, thereby stirring the suspension of dust particles. This result provides an experimental verification, for the field of fluid mechanics, that TCF in the slip-flow regime causes steady-state gas flow in a confined volume.

DOI: 10.1103/PhysRevE.80.046402 PACS number(s): 52.27.Lw, 47.45.Gx, 47.80.Jk

I. INTRODUCTION

Thermal creep flow (TCF) is a flow of gas driven by a gas temperature gradient along a solid boundary. Since gas flows along the boundary, TCF is very different from the usual no-slip boundary conditions used in the Navier-Stokes model of gas (fluid) flow. The width of this boundary flow is on the order of a gas mean free path λ.

Although TCF occurs near a solid boundary, it does influence gas flow in other regions. As a result of collisions between neutral gas atoms, the *boundary* gas flow TCF can still drive a slower flow of the *bulk* gas. Here, bulk gas refers to gas in a region that is many mean free paths from the solid boundary. Faster atoms near the boundary can transfer momentum to atoms in the bulk gas via collisions, resulting in a directed flow of the bulk gas.

The effect of TCF was discovered by Reynolds [1] and then theoretically quantified by Maxwell in the last year of his life [2]. Today, industrial applications that exploit TCF include chemical vapor deposition in integrated circuit fabrication [3] and crystal growth [4]. Despite the importance of these applications, experiments to detect TCF are rare [5–7]. The literature for TCF mostly consists of reports of numerical simulations [8–15].

Observing TCF experimentally poses a number of challenges. This kind of flow occurs within a few mean-free paths of a heated surface. At atmospheric pressure it would be limited to micron-size regions, which are too small for most flow detection schemes. This size limitation can be relaxed by making measurements under vacuum conditions, where mean-free paths are larger, but fewer sensors are practical. When it is impractical to position a sensor within a few mean-free paths of a surface, one must measure the flow of bulk gas that is driven by TCF, yielding an indirect detection of TCF.

The earliest experiment designed to detect TCF was performed using a windmill as a sensor and a bell jar to provide vacuum conditions [5,6]. The heated surface was a glass plate. The mean-free path was <1 mm, much smaller than the windmill. The windmill was located 11 mm from the glass plate. Although the authors in Refs. [5,6] did not discuss TCF and flow of bulk gas separately, we can interpret their experiment as detecting flow in the bulk gas because the sensor was located many mean free paths from the surface. Thus, their results rely on recognizing that a flow of bulk gas can be driven by TCF. Moreover, other causes of bulk gas flow, such as free convection, must be eliminated. The windmill experiment was designed so that the effects of free convection could be contrasted with those of TCF.

Dusty plasma is a suspension of small micron-size dust particles in a background of electrons, ions, and neutral gas. The dust becomes charged by absorbing electrons and ions. Dusty plasma is of special importance in industrial applications such as semiconductor manufacturing [16,17] as well as in astrophysics [18].

The dusty plasma literature has long recognized the importance of the thermophoretic force in both experiment [19,20] and theory [21], but it has only recently recognized TCF [7]. As our main result, we report an experiment verifying the recent discovery [7] that TCF can have a large effect on dusty plasma. Our result also serves as a rare experimental demonstration of TCF, for the fluid mechanics community. In both experiments (here and in Ref. [7]) nonuniform temperature gradients are purposefully set up to drive TCF, evidenced by the effect this gas flow has on dusty (complex) plasma.

Dust particles can be confined indefinitely in a plasma. This confinement is accomplished by forces acting on the dust particles in the plasma. In the vertical direction, the downward forces of gravity and the ion drag force are balanced by an upward electric force due to a natural electric field in the plasma, which is sometimes augmented by an upward thermophoretic force [20]. In the horizontal direction, the mutually repulsive forces between negatively charged particles are balanced by natural horizontal electric forces.

Additional forces, for example due to gas flow, can set dust particles into motion while confinement forces prevent their escape. Here, the result of additional forces can have two observable effects: the entire suspension can be *displaced* to a new equilibrium position, and the dust suspension can be *stirred* so that dust particles circulate within the suspension. In this paper, it will be argued that an overall displacement indicates a conservative force, whereas an observation of stirring indicates the presence of a gas flow.

We will use the visible motion of dust particles suspended in a dusty plasma as an indicator of TCF. Because of their small mass and lack of frictional contact with solid surfaces, dust particles move easily in response to ambient gas flow and small forces. The dust suspension will serve the same purpose as the windmill in Ref. [5], as both are set in motion by local flow of the bulk gas.

II. NEUTRAL GAS FLOW AND TEMPERATURE GRADIENTS

Transport processes in gas are classified into flow regimes, distinguished according to the dimensionless Knudsen number, Kn. The Knudsen number is the ratio of the mean free path λ to a characteristic scale length L, and its value indicates the importance of molecular collisions. Thermal creep flow (TCF) is most prominent in the *slip-flow regime* ($10^{-3} < \mathrm{Kn} < 0.1$), where, due to the dominance of collisions, the gas can be treated as an infinitely divisible fluid, but only with appropriate boundary conditions. By performing our experiment under vacuum conditions, with surfaces at a centimeter length scale, we assure that gas flow is in the slip-flow regime.

Thermal creep gas flow results from a nonuniformly heated gas being in contact with a solid surface. A temperature gradient with a component tangential to the surface drives a gas flow. The flow velocity is directed toward hotter gas regions and is largest at the gas-surface interface. In this way, TCF is a *boundary* effect.

The TCF effect depends strongly on the Knudsen number. In the slip-flow regime, where TCF is most important, the TCF gas flow velocity, tangential to the boundary at the boundary surface, is [22] $v_{creep} = \omega(2k_B T/m)^{1/2}\mathrm{Kn}_T$. This is valid within a distance λ of the boundary, and not in the bulk gas. Here, ω is a constant of order unity, k_B is Boltzmann's constant, T is the gas absolute temperature, and m is gas atom mass. Note that v_{creep} is proportional to the Knudsen number on the scale of the gas temperature gradient, Kn_T, revealing that TCF is more significant at larger mean free paths, or lower pressures, as was verified experimentally [5]. Here, $\mathrm{Kn}_T \equiv (\lambda/T)(dT/dx)$, and (dT/dx) is the tangential component of the gas temperature gradient evaluated at the boundary.

Conditions that lead to TCF will often be accompanied by two other effects: a thermophoretic force and free convection. All three effects result from a temperature gradient. To design an experiment that allows distinguishing these effects requires careful planning. We next review the thermophoretic force and free convection, before presenting the design of our experiment.

The thermophoretic force $\vec{F}_{th}$ arises when a small dust particle (usually microns or smaller in size) is exposed to a nonuniformly heated gas. Dust particles are pushed toward colder gas regions. This happens because a gas temperature gradient causes an anisotropy in the gas velocity distribution function, which in turn causes more momentum to be imparted to dust from hot gas regions than from cold gas regions [23]. For a spherical particle in an unequally heated background of argon gas [20], $\vec{F}_{th} = 3.33(R^2/\sigma)k_B(-\vec{\nabla}T)$, where R is the dust particle's radius and σ is the collision cross section for argon atoms. Note that unlike TCF, the thermophoretic force does not require a boundary, and it does not necessarily involve a gas flow. It involves a gradient of the gas temperature in a volume of gas, while TCF involves a tangential temperature gradient on a boundary.

Free convection is a gas flow driven by buoyancy when there is a temperature gradient. It requires a body force, such as gravity, that is aligned with the temperature gradient. Gravity, in combination with gas density gradients that arise from temperature gradients, leads to the gas flow. Hotter gas regions expand and rise, where they are then cooled. Colder gas regions condense and fall, where they are then heated. Free convection is often characterized by the dimensionless Rayleigh number, which is generally interpreted as the ratio between buoyancy forces and viscous forces.

III. EXPERIMENTAL DESIGN

We performed an experiment designed especially to detect TCF, and to isolate its effects. We use a *locally heated* solid boundary to cause temperature gradients that drive gas flow. Dust particles serve as indicators of gas flow.

The design of the experiment isolates TCF from most other processes, except for the thermophoretic force and free convection. Thus, our experimental design will allow a conclusion that we have detected TCF if we can distinguish it from the thermophoretic force and free convection. We will be able to do this because the thermophoretic force has a signature that is different from that of TCF, as we explain later. Free convection is ruled out two ways: a theoretical argument based on the Rayleigh number for our experimental conditions, and by comparing the horizontal and vertical dust kinetic energy in our experimental data.

We compare and contrast our experiment's design to that of Ref. [7]. Both experiments isolate the effect of TCF, and enable detecting very slow gas flow by avoiding vertical dust sedimentation. Our heat source is designed to drive TCF mostly *perpendicular* to gravity. Because our heat source is *independent* of the forces that confine dust, the effect of gas flow driven by TCF is then very clear since it disturbs the equilibrium. In Ref. [7], bulk gas flow driven by TCF is aligned *antiparallel* to gravity and also contributes to dust confinement. The design of their experiment allowed for calculation of the *gas flow* velocity field, as well as comparison to theory.

A. Apparatus

Our apparatus makes use of a radio-frequency (rf) gas discharge plasma in a vacuum chamber. Polymer microspheres (dust particles) are injected [24], become electrically charged, and are levitated as a three-dimensional (3D) suspension called a Coulomb ball or Yukawa ball [25]. This suspension is confined in equilibrium within the volume of a glass box. This equilibrium is purposely disturbed by *locally* heating the glass box to drive TCF, as described later.

The Yukawa ball's equilibrium is maintained by a configuration of forces. In the vertical direction, the electric

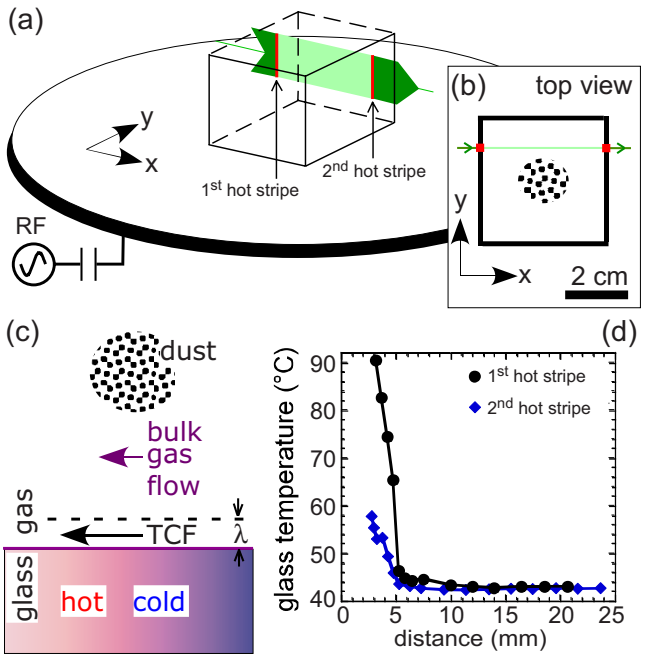

FIG. 1. (Color online) (a) Perspective view (dust not shown) and (b) top view (dust shown) of how a vertical laser sheet (broad arrow) is used to heat two stripes on a glass box. The laser sheet strikes two faces of the box, creating two heated stripes (shown in red and indicated with two arrows), but does not strike dust. The laser sheet is shown both in the interior (light green) and exterior (dark green) of the box. (c) Sketch of gas flow arising from tangential temperature gradients at a glass-gas boundary. In the rarefied gas near the boundary, TCF occurs; this couples to the bulk gas farther from the boundary, causing it to flow also. Flow of the bulk gas disturbs the dust suspension, which we image. (d) Glass temperature, measured under the same vacuum conditions but without plasma, vs horizontal distance from each of two heated stripes.

force and a thermophoretic force balance gravity and ion drag. In the horizontal direction, the electric force balances interparticle repulsion between negatively charged dust particles. The electric force is set up by applying a few Watts of rf power to the lower electrode. The upward thermophoretic force is set up by *uniformly* heating this lower electrode.

The glass box plays two roles. First, it serves as a boundary that we heat using a laser. Second, the glass box provides horizontal confinement of the dust suspension, because the dielectric walls of the box modify the plasma's natural electric field [26]. The glass box rests atop the lower electrode, is open on top and bottom, and partially encloses a volume of $(40\ \text{mm})^3$ as in Fig. 1(a). The box is constructed from four glass plates $(40\times40\times1.5\ \text{mm}^3)$ that are glued together at their edges.

There are a few required conditions to be met in order to observe TCF in dusty plasma. First, TCF is most readily observed in the slip-flow regime. Second, TCF requires a gas temperature gradient tangential to a solid surface. Finally, the flow of gas must be detectable, which can be difficult because it is a low Mach number flow. Next, we describe how the design of our experiment meets these conditions.

The parameters for the gas and the glass box assure us that gas flow inside the box is in the slip-flow regime. We use argon at 0.4 Torr, corresponding to $\lambda=0.12$ mm. For the box with $L=40$ mm, we find $\text{Kn}=0.003$, which is at the lower limit for the slip-flow regime.

B. Localized heating

To detect TCF in isolation from other effects, it is desirable to have a heat source that does not disturb the electrical configuration of the plasma. As an optical solution, we used a 3 W 532 nm cw laser beam to *locally* heat two sides the glass box. The box absorbs some of the laser radiation. The laser is useful for heating glass, but not powerful enough to cause significant laser-plasma interactions with electrons and ions.

We want temperature gradients due to laser heating to be mostly in the *horizontal* plane, for two reasons. First, forces that confine dust in equilibrium are weaker in the horizontal direction, as compared to the vertical direction. Thus, additional forces that *disturb* dust equilibrium (including $\vec{F}_{th}$ and gas drag) have the greatest effect on a dust particle if they are directed horizontally. Second, driving dust motion horizontally helps distinguish TCF from free convection, which should effect dust motion mainly in the vertical plane.

To produce mostly *horizontal* temperature gradients, the laser beam is rastered [27] into a vertical sheet of laser light 16 mm high and 1 mm wide. It passes through two sides of the glass box, locally heating two stripes, as in Fig. 1(a) and 1(b). The laser is directed so that dust particles are not struck by the primary beam or any weaker reflected beams.

Since TCF is generated at boundaries, we identify the boundaries in our experiment that are heated. The glass box is *locally* heated in two vertical stripes. The only other nearby boundary is the lower electrode, which is large (17-cm diameter), and is *uniformly* heated. Thus, only the glass boundaries are expected to have a significant tangential temperature gradient, as required to drive TCF.

To clearly demonstrate the effect of our heat source, we perform two types of tests with dusty plasma, one using a heated box and the other using a control box. The heated box is made of common window glass, and it is heated by absorbing laser radiation. The control box (similar in size to the heated box) is made of fused silica, which has almost negligible absorption, so that it is not heated by laser radiation. All other conditions, including the ambient gas flow to the vacuum pump, are the same for the control. More detail is given in Sec. IV.

C. Detecting gas flow with dusty plasma

A suspension of microspheres in the dusty plasma is used to diagnose gas flow. Our method of detecting TCF is to observe the motion of dust particles accelerated by flow of the bulk gas, which is driven by TCF at the boundary, as sketched in Fig. 1(c). To do this, we track the motion of individual dust particles by imaging either a horizontal plane from above, or a vertical plane from the side. We use a digital camera at 53 frames per second. Micron-sized or larger particles are easiest to identify individually; here, we use 4.8 μm microspheres.

Our method of detecting TCF differs from previous methods used in fluid mechanics experiments. Unlike in Ref. [5], where a windmill provided a single-point measurement of flow in a rarefied gas, here we use dust particles embedded in the gas to indicate gas motion everywhere within the volume of the dust suspension. This use of dust particles resembles velocimetry methods commonly used in fluid mechanics, except that we have other vertical forces to offset gravity and avoid sedimentation.

To identify the effect of a drag force due to gas flow (driven by TCF or free convection) we must be able to distinguish it from the effect of the thermophoretic force $\vec{F}_{th}$, which inevitably will also occur. Here, a signature of a drag force is a steady-state flow of dust. Since $\vec{F}_{th} \propto \vec{\nabla} T$, it is a *conservative* force, and the work done by $\vec{F}_{th}$ on a dust particle around a closed loop is $\oint \vec{F}_{th} \cdot d\vec{x} = 0$. Thus, $\vec{F}_{th}$ cannot drive a steady-state flow of dust because it cannot add energy to the system. The drag force on a dust particle, however, is proportional to a velocity and is *nonconservative*, thus $\oint \vec{F}_{drag} \cdot d\vec{x} \neq 0$. A steady flow of gas can drive dust particles into a steady-state flow. In our experiment, we exploit this to distinguish the effects of a drag force from $\vec{F}_{th}$.

D. Temperature measurements

In a test with the same vacuum conditions mentioned above, but without plasma, we characterized the temperature gradients of the heated glass boundary. Using a thermocouple, we measured the *horizontal* profiles of glass temperature due to the laser heating two faces of the glass box. This is done by holding fixed the position of the thermocouple and varying the position of the laser beam [28]. The result is glass temperature plotted vs distance from the heat source for each heated stripe, Fig. 1(d). The heating of the glass had a time scale of ≈ 60 s, during which most of the observed temperature increase occurred.

Knowing the temperature gradient allows us to estimate $\vec{F}_{th}$ and v_{creep}. These quantities depend on temperature gradients at different locations: v_{creep} depends on the tangential component of the temperature gradient at the glass boundary while $\vec{F}_{th}$ depends on the temperature gradient in the bulk gas, where dust particles are located. In Fig. 1(d), the temperature gradient varies from 16 K/mm at a distance of 4 mm from the heat source to 0.2 K/mm at 20 mm from the heat source. Using these measurements, the *horizontal* bulk gas temperature gradient was calculated as ≥ 0.2 K/mm (this should not be confused with the uniform *vertical* temperature gradient which contributes to equilibrium). Using this value, we estimate $\vec{F}_{th}$ on one particle due to laser heating to be $\geq 1.2 \times 10^{-13}$ N. This is about one eighth the force of gravity, which is 8.6×10^{-13} N. Using the larger value for the temperature gradient, we predict v_{creep} near the heated glass to be ≤ 2 m/s.

IV. RESULTS

In excluding all alternative explanations for our results, other than TCF, our logic will have three steps. First, we will explain how the dust motion has been demonstrated to arise from temperature gradients. Second, we will explain how the stirring motion of dust must be due to a coupling between dust and a flow of gas (not $\vec{F}_{th}$). Third, we will eliminate free convection as a possibility, leaving us with TCF as the only explanation for our results.

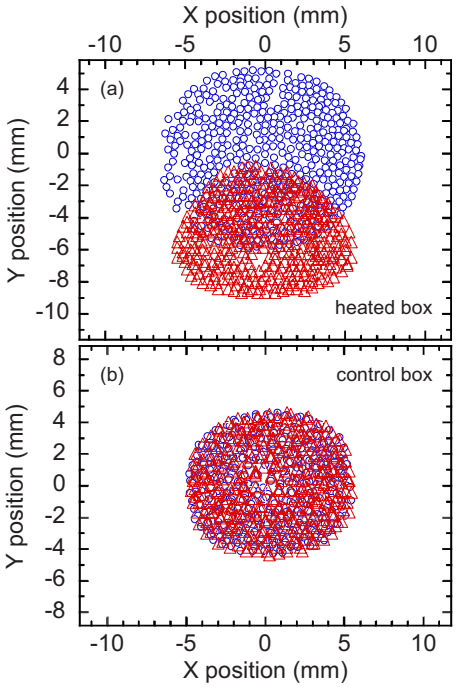

FIG. 2. (Color online) Top view of dust particle positions, from separate tests using (a) the heated box that absorbs light and (b) the control box that does not absorb light. Each panel shows dust particle positions in a horizontal plane before laser application (blue circles) and during laser application (red triangles). The origin is the horizontal center of the glass box. A laser sheet strikes the two faces of the box, as in Figs. 1(a) and 1(b). In the test with the heated box, the dust suspension (Yukawa ball) is *displaced* away from the heating laser beam to a new *horizontal* equilibrium position. This displacement is attributed to the thermophoretic force.

A. Plasma effects vs temperature gradients

In our main experiment with plasma, we first compare results of tests with the heated and control boxes (Fig. 2). In each test, as explained in Sec. III, a 3D dusty plasma (Yukawa ball) is confined within the volume of the glass box. A single laser strikes two faces of the glass box, as in Fig. 1, and any resulting dust motion is monitored from above. Any differences in the results for the two tests must be attributed to heat due to laser-light absorption in the common window glass of the heated box. Plasma forces such as the electric force and the ion drag force cannot be responsible because the plasma's electrical conditions are not altered by our laser heating method. Because the laser never directly strikes dust, there is no radiation pressure force affecting dust motion. The force of gravity acts perpendicular to the horizontal viewing plane. Finally, any gas drag force due to ambient gas flow to the vacuum's pump is the same for the heated and control boxes.

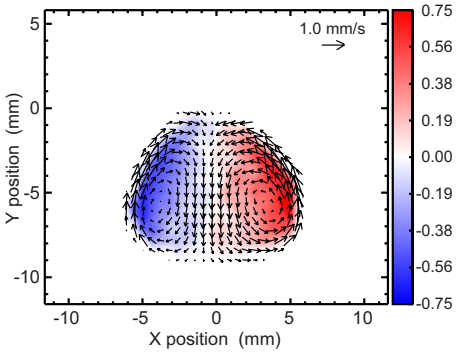

FIG. 3. (Color online) Top view of the steady-state dust velocity field $\vec{V}$ (black arrows) and vorticity $\vec{\nabla}\times\vec{V}$ (color map) in units of s^{-1}. Gravity is into the page. The origin is the equilibrium center of the Yukawa ball. Data shown are dust velocities mapped to a regular grid (40×30), and averaged over the movie's last 100 frames. The stirring of dust into a horizontal flow is our main result that we seek to explain.

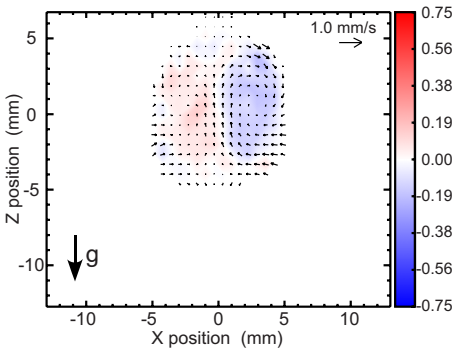

FIG. 4. (Color online) Side view of the steady-state dust velocity field $\vec{V}$ (black arrows) and vorticity $\vec{\nabla}\times\vec{V}$ (color map) in units of s^{-1}. Gravity is directed downward. The origin is the equilibrium center of the Yukawa ball. Data shown are averaged and scaled as in Fig. 3. Comparing to Fig. 3 shows that the flow of dust is predominantly horizontal, indicating that the flow of bulk gas is also predominantly horizontal.

Results shown in Fig. 2 and 3 establish that a temperature gradient drastically disturbs the Yukawa ball. Particle positions before laser application (blue circles) and during laser application (red squares) are shown in Fig. 2, for tests using both the heated box and the control box. While the Yukawa ball in the control box showed no change when the laser beam was applied [Fig. 2(b)], the Yukawa ball in the heated box changed in two ways: it was displaced and it rotated. In Fig. 2(a), the suspension is displaced away from the heat source by a distance of about 6 mm, which is over half the size of the Yukawa ball. The steady-state flow of dust for the test using a heated box is shown in Fig. 3, with arrows indicating dust velocity and a color map indicating dust vorticity. The suspension rotates into a steady state, as if being stirred, with the fastest particles at the edge and slower particles in the interior. Thus, we conclude that the dust motion that ensues when the laser strikes the box is attributed to resulting gas temperature gradients and not to any plasma forces.

B. Thermophoretic force vs gas drag force

The displacement of the Yukawa ball is due to $\vec{F}_{th}$. Dust is pushed away from the heat source toward colder gas regions, consistent with the direction of $\vec{F}_{th}$. The estimate above for the magnitude of $\vec{F}_{th}$ is large enough to account for the Yukawa ball's displacement, based on the force calculations of Arp *et al.* [26].

The steady-state rotational flow of dust particles is due to coupling between dust and a flow of gas, or gas drag. The observation of a steady-state flow (shown in Fig. 3) is a signature that rules out $\vec{F}_{th}$, as argued in Sec. III, based on the conservative nature of $\vec{F}_{th}$. A movie showing the temporal development of the dust velocity field, as it approaches steady state, can be viewed in Ref. [28].

C. Thermal creep flow vs free convection

At this point, we have demonstrated that the stirring motion of the dust is due not to plasma effects but rather to temperature effects, and we have eliminated the thermophoretic force as a candidate for explaining the stirring. The two effects that remain to consider are TCF at the glass boundary and vertical free convection due to gas buoyancy.

Next, we will eliminate free convection as an explanation of our stirring observations, for two reasons. First, we estimate the Rayleigh number and find that it is much too low for free convection. Second, we will compare the dust kinetic energies associated with horizontal and vertical motion. Vertical motion is of interest for free convection because buoyancy drives vertical motion, which can then couple to horizontal motion.

First, we compare the Rayleigh number in our experiment to the critical Rayleigh number for the onset of buoyancy-driven flow (free convection). For our experimental conditions, we estimate the Rayleigh number to be 0.1. This is much lower than the *critical* Rayleigh number, above which free convection becomes important. The critical Rayleigh number is 1708 [29,30]. Thus, we suspect that free convection is not significant in our experiment.

Second, we compare horizontal and vertical dust motion. To do this, we observed dust motion from both the top and the side, using the same camera in separate runs. The steady-state dust velocity map in the *horizontal* plane is shown in Fig. 3. For comparison, the steady-state dust velocity map in the *vertical* plane is shown in Fig. 4. In order to compare scalar quantities, we compared the kinetic energy associated with horizontal velocity components to the kinetic energy associated with vertical velocity components. We performed five runs viewing from the top, and two from the side. All runs showed a clear increase in dust kinetic energy that coincided with the onset of laser heating, and eventually reached a steady-state energy. For both horizontal and vertical motion, there was a slight variation in the steady-state energy from run to run. The average steady-state energy for *horizontal* motion for five runs was $(4.4\pm1.4)\times10^{-21}$ J, while the average steady-state energy for *vertical* motion for two runs was $(5.3\pm1.3)\times10^{-22}$ J. The time series for these kinetic energies is shown in Fig. 5, with black circles show-

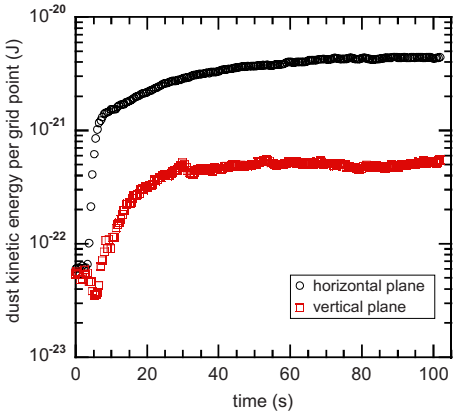

FIG. 5. (Color online) Time series of kinetic energy of dust particles in a horizontal plane averaged over five runs (black circles) and of particles in a vertical plane averaged over two runs (red squares). The laser heating is applied at $t=5$ s. Dust motion in the vertical direction is much weaker than in the horizontal. The comparison of vertical vs horizontal motion here and in Fig. 4 leads us to eliminate free convection as the cause of the observed stirring in Fig. 3. Each datum is averaged over all nonzero gridpoints in the 40×30 field of view and then over 100 contiguous frames (2 s).

ing energy in the horizontal plane and red squares showing energy in the vertical plane. Laser heating begins at $t=5$ s, and remains on for the remainder of the time series. At all times after heating began, kinetic energy associated with vertical motion was nearly a factor of ten less than horizontal motion. Dust energy reaches a steady state about 1 min after laser heating begins, the same as the time scale for laser heating, as mentioned in Sec. III.

We conclude that steady-state stirring of the dust suspension is not due to free convection, leaving TCF as the only explanation. We know that the gas flow is not driven by free convection because horizontal dust motion had nearly a factor of ten more energy than vertical motion, as shown in Fig. 5. This is further supported by our earlier estimate for the Rayleigh number.

V. SUMMARY

We performed an experiment with a dusty plasma that was designed to observe TCF, in isolation from other effects, as described in Sec. III. We observed a stirring motion in the confined dust suspension. This stirring motion developed as two glass boundaries heated up, due to applying a laser beam. In Sec. IV, we presented our logic to dismiss, in three steps, all alternative effects that might account for our observations of stirring. First, a test with a control box allowed us to conclude that we can eliminate from consideration all plasma-related forces that are not associated with temperature gradients. Second, by noting that stirring motion requires a nonconservative force, we eliminated the thermophoretic force as an explanation. Third, we eliminated free convection two ways: finding that our Rayleigh number was much too small, and by comparing the vertical and horizontal motion. We therefore conclude that the stirring we observed results from the flow of bulk gas, which is driven at the boundaries by TCF.

This experimental test serves two purposes, for two different scientific communities. For the fluid mechanics community, it serves as a rare experimental verification of the existence of TCF. For the plasma physics community, it verifies the recently reported demonstration [7] that TCF can have a significant effect on dusty plasmas. Our experiment differs from the one used in Ref. [7] in several ways, including our configuration designed so that TCF results in a horizontal flow to allow distinguishing it from convection, and an optical method of heating a boundary.

ACKNOWLEDGMENTS

This work was supported by NASA and DOE. The authors thank O. Arp for instruction and helpful discussions.

[1] O. Reynolds, Philos. Trans. R. Soc. London **170**, 727 (1879).
[2] J. C. Maxwell, Philos. Trans. R. Soc. London **170**, 231 (1879).
[3] D. W. Hess and K. F. Jensen, *Microelectronics-Processing Chemical Engineering Aspects* (American Chemical Society, Washington, D.C., 1989), p. 203.
[4] S. Musso *et al.*, J. Cryst. Growth **310**, 477 (2008).
[5] Y. Sone, Phys. Fluids A **3**, 997 (1991).
[6] Y. Sone, K. Sawada, and H. Hirano, Eur. J. Mech. B/Fluids **13**, 299 (1994).
[7] S. Mitic, R. Sutterlin, A. V. Ivlev, H. Hofner, M. H. Thoma, S. Zhdanov, and G. E. Morfill, Phys. Rev. Lett. **101**, 235001 (2008).
[8] T. Ohwada, Y. Sone, and K. Aoki, Phys. Fluids A **1**, 1588 (1989).
[9] T. Ohwada, Y. Sone, and K. Aoki, Phys. Fluids A **1**, 2042 (1989).
[10] S. K. Loyalka, Phys. Fluids A **1**, 403 (1989).
[11] D. H. Papadopoulos and D. E. Rosner, Phys. Fluids **7**, 2535 (1995).
[12] K. Sugiyama *et al.*, JSME Int. J., Ser. B **39**, 376 (1996).
[13] Y. Sone, Annu. Rev. Fluid Mech. **32**, 779 (2000).
[14] C. E. Siewert, Phys. Fluids **15**, 1696 (2003).
[15] S. Takata, S. Yasuda, S. Kosuge, and K. Aoki, Phys. Fluids **15**, 3745 (2003).
[16] G. S. Selwyn, J. Singh, and R. S. Bennett, J. Vac. Sci. Technol. A **7**, 2758 (1989).
[17] B. M. Jelenković and A. Gallagher, J. Appl. Phys. **82**, 1546 (1997).
[18] C. K. Goertz, Rev. Geophys. **27**, 271 (1989).
[19] G. M. Jellum, J. E. Daugherty, and D. B. Graves, J. Appl. Phys. **69**, 6923 (1991).
[20] H. Rothermel, T. Hagl, G. E. Morfill, M. H. Thoma, and H. M. Thomas, Phys. Rev. Lett. **89**, 175001 (2002).
[21] O. Havnes *et al.*, Plasma Sources Sci. Technol. **3**, 448 (1994).
[22] C. Cercignani, *Theory and Application of the Boltzmann Equation* (Scottish Academic Press Ltd., 1975), Chap. 5, p. 255.

[23] L. Talbot *et al.*, J. Fluid Mech. **101**, 737 (1980).
[24] M. Mikikian *et al.*, New J. Phys. **5**, 19 (2003).
[25] O. Arp, D. Block, A. Piel, and A. Melzer, Phys. Rev. Lett. **93**, 165004 (2004).
[26] O. Arp *et al.*, Phys. Plasmas **12**, 122102 (2005).
[27] V. Nosenko, J. Goree, Z. W. Ma, and A. Piel, Phys. Rev. Lett. **88**, 135001 (2002).
[28] See EPAPS Document No. E-PLEEE8-80-063910 for two movies and further detail about apparatus. For more information on EPAPS, see http://www.aip.org/pubservs/epaps.html.
[29] L. D. Landau and E. M. Lifshitz, *Fluid Mechanics* (Pergamon Press, New York, 1987), Chap. 5, p. 225.
[30] J. K. Bhattacharjee, *Convection and Chaos in Fluids* (World Scientific Publishing, Singapore, 1987), Chap. 1, p. 8.